J Eng Math (2007) 59:399–417
DOI 10.1007/s10665-007-9173-3

A multiple-scales approach to crack-front waves

Andrew N. Norris · I. David Abrahams

Received: 25 June 2007 / Accepted: 5 July 2007 / Published online: 2 August 2007

Abstract Perturbation of a steadily propagating crack with a straight edge is solved using the method of matched asymptotic expansions (MAE). This provides a simplified analysis in which the inner and outer solutions are governed by distinct mechanics. The inner solution contains the explicit perturbation and is governed by a quasi-static equation. The outer solution determines the radiation of energy away from the tip, and requires solving dynamic equations in the unperturbed configuration. The outer and inner expansions are matched via the small parameter $\epsilon = L/l$ defined by the disparate length scales: the crack perturbation length L and the outer length scale l associated with the loading. The method is illustrated for a scalar crack model and then applied to the elastodynamic mode I problem. The crack-front wave-dispersion relation is found by requiring that the energy release rate is unaltered under perturbation and dispersive properties of the crack-front wave speed are described for the first time. The example problems considered demonstrate the potential of MAE for moving-boundary-value problems with multiple scales.

Keywords Crack-front waves · Crack propagation · Dynamic fracture · Matched asymptotic expansions · Multiple scales · Wiener–Hopf

1 Introduction

Dynamic perturbation of a steadily travelling crack in a linear elastic medium is of fundamental interest in fracture mechanics. The possible existence of edge-supported modulations in an otherwise straight edge raises questions about the stability of a steadily moving crack front. These waves, called crack-front waves, have been the subject of intense scrutiny since they were first observed by Rice et al. [1] and Perrin and Rice [2] through numerical simulations of interactions of dynamic crack fronts with inhomogeneities. A theoretical framework for crack-front waves was provided by Ramanathan and Fisher [3] using dynamic weight functions derived earlier by Willis and Movchan [4]. Ramanathan and Fisher [3] showed that a mode I (opening) disturbance can propagate along the

A. N. Norris (✉)
Department of Mechanical & Aerospace Engineering, Rutgers University, Piscataway, NJ 08854, USA
e-mail: norris@rutgers.edu

I. D. Abrahams
University of Manchester, Oxford Road, Manchester M13 9PL, UK
e-mail: i.d.abrahams@manchester.ac.uk

crack front with a speed that is a function of the crack velocity and less than the Rayleigh-wave velocity. Further numerical work confirmed the earlier findings [5] and showed the explicit form of the (non-dispersive) crack-front wave speed as a function of the crack speed v [6,7].

The theory of Willis, Movchan and Ramanathan has been extended to other configurations and experimentalists have sought evidence of crack-front waves. Woolfries and Willis [8] gained insight by examining a scalar crack model. Woolfries et al. [9] generalised the dynamic weight-function method to cracks in viscoelastic materials which was used by Willis and Movchan [7] to show that crack-front waves decay in the presence of viscoelasticity. These theoretical studies considered perturbations of the crack edge in the plane of the moving crack. Obrezanova et al. [10,11] examined out-of-plane perturbations of a 2-dimensional crack, and Movchan et al. [12] considered the dynamic stability of a crack in a strip. Predictions of crack-front waves have also been investigated through experiments. Crack-front waves have been proposed as the cause of crack-surface roughening in brittle materials [13]. Sharon et al. [14–16] claim to have evidence of crack-front waves in several experiments. Their conclusions are at odds with those of Bonamy and Ravi-Chandar [17] who used ultrasonic shear waves to distort dynamically growing cracks. They found that the perturbation of the crack front is a linear function of the wave amplitude, but the crack perturbation does not persist after the exciting wave has passed. Many questions on crack-front waves remain to be answered.

The purpose of this paper is to present a new, and, as we will argue, simpler, method for analysing the problem of a perturbed dynamic crack. The basic idea is that the size of the crack-front disturbance is small compared with a macroscopic length scale, which we choose here to be defined by the dynamic loading. These yield inner and outer length scales and a small parameter ϵ which is the ratio of the length scales. Our approach uses the method of matched asymptotic expansions (MAE) to split the elastodynamic problem into inner and outer sub-problems each of which is simpler than the entire problem and contains the physics appropriate to the region. As we will demonstrate, the inner problem is quasi-static and depends explicitly on the assumed form of the crack perturbation. The outer problem does not consider the fine scale of the perturbation directly, although it determines the radiation of energy from the inner region. The inner and outer solutions are related to one another through standard matching arguments. While the use of asymptotic methods in fracture mechanics is certainly not new, e.g. [18], the method of MAE has not been used for dealing with complex moving-boundary-value problems of the type considered here. MAE is both useful and productive for this class of problem as it naturally splits the problem mechanically and mathematically.

The layout of the paper is as follows. We begin in Sect. 2 with a model problem demonstrating the matched asymptotic approach to studying the perturbation of a travelling crack edge. The steady solution and the scaling for the perturbation are introduced in Sect. 2, and the details of the MAE analysis are given in Sect. 3. The same approach is then applied in Sect. 4 to the physically realistic case of a mode I crack travelling in an elastic material. The scaling, matching procedure and total solution for the elastodynamic case are developed in a manner analogous to the scalar problem. The crack-front wave-dispersion relation is obtained and new results are presented for the dispersive behaviour of the crack-front wave speed, with numerical examples given in Sect. 5.

2 The scalar model problem of a travelling crack

In this section a model elastic problem of a dynamic perturbation to a travelling crack front is solved using MAE. The application is similar to that for the elastic crack but less complex. We therefore present it in detail in order to illustrate the general procedure.

2.1 Non-dimensional parameters and scaling

Consider a function $\phi(x, y, z, t)$, motivated by the anti-plane displacement field in mode III elasticity [1], and satisfying a scalar wave equation

$$\nabla^2\phi - c^{-2}\phi_{tt} = 0, \tag{1}$$

where ∇^2 is the Laplacian operator, the subscript t denotes partial differentiation in time, and c is the speed of acoustic waves. A crack occupies the region

$$x < vt + Lf(z,t), \qquad y = 0, \quad -\infty < z < \infty, \tag{2}$$

that is, it grows at a constant speed, v, except for a perturbation term Lf, where the length L is the magnitude of the deviation and f is a dimensionless $\mathcal{O}(1)$ quantity. For purely out-of-plane motions (displacement in the z-direction) the crack faces carry zero stress, which we model here (see [1]) as

$$\phi_y(x,0,z,t) = 0, \quad x < vt + Lf, \tag{3}$$

where $\phi_y = \partial\phi/\partial y$, etc. The crack therefore opens at a rate that is approximately constant, and it is the deviation from the steady state that is of interest. The opening is assumed to be caused by a steadily translating symmetric loading on the crack faces,

$$\phi_y(x,\pm 0,z,t) = \frac{P}{l}\, p\left(\frac{x-vt}{l}\right). \tag{4}$$

Note that we have assumed that the non-dimensional forcing function p has argument that scales on a length scale l, which is taken to be *much larger* than the perturbation scale L. (For simplicity we interpret this to also imply that $p(x)$ is zero in the vicinity of the crack tip.) We define the small parameter ϵ as the ratio of the two length scales:

$$\epsilon = L/l. \tag{5}$$

It is convenient to move to a coordinate system fixed in the (constant) moving reference frame, and to non-dimensionalise the initial-boundary-value problem. Thus, we define dimensionless independent variables as

$$\frac{x-vt}{l} \to x, \quad \frac{y}{l} \to y, \quad \frac{z}{l} \to z, \quad \frac{ct}{l} \to t, \tag{6}$$

together with

$$\frac{v}{c} \to v, \quad \frac{\phi}{P} \to \phi, \tag{7}$$

and the problem reduces to analysing the system

$$\alpha^2\phi_{xx} + \phi_{yy} + \phi_{zz} - \phi_{tt} + 2v\phi_{xt} = 0, \tag{8a}$$

$$\phi_y(x,\pm 0,z,t) = p(x), \quad x < \epsilon f(z,t), \tag{8b}$$

where

$$\alpha = \sqrt{1-v^2}\,. \tag{9}$$

The loading function $p(x)$ is, by definition, zero close to the crack tip, and we assume that the crack-growth speed is subsonic so that α remains real. The system (8) still needs to be supplemented by a crack-growth criterion, discussed below. We emphasise that here and henceforth all parameters and variables are non-dimensional.

2.2 Constant running crack

It will prove useful later to first consider the solution to (8) for zero perturbation in the crack-tip position, $f(z,t) = 0$. We start with a constant running point loading applied symmetrically to the crack faces at distance unity (i.e., at distance l in the original coordinate system) behind the crack tip:

$$\phi_y(x,\pm 0,z) = \delta(x+1), \quad x < 0. \tag{10}$$

Here $\delta(x)$ is the Dirac delta function. Note that, with a symmetric loading, ϕ will be zero ahead of the crack tip, and so this is a standard two-part boundary-value problem which may be solved in a variety of ways; a solution of (8) and (10) is therefore

$$\phi_y(x,y,z) = \mathfrak{Re}\left\{\frac{-1}{\pi(x+\mathrm{i}\alpha y+1)\sqrt{x+\mathrm{i}\alpha y}}\right\}. \tag{11}$$

It may be checked, using the identity $(x-\mathrm{i}0)^{-1}-(x+\mathrm{i}0)^{-1}=2\pi\mathrm{i}\delta(x)$, that (11) indeed satisfies (10). Expanding about the crack tip, and integrating, we find the solution for ϕ as

$$\phi(x,y,z,t)=\Im\mathfrak{m}\left\{\frac{-1}{\pi\alpha}\sum_{n=0}^{\infty}\frac{(-1)^n}{n+\frac{1}{2}}\,(x+\mathrm{i}\alpha y)^{n+\frac{1}{2}}\right\}. \tag{12}$$

Note that in (11) and (12), $\Re\mathfrak{e}$ and $\Im\mathfrak{m}$ denote the real and imaginary parts of the expressions to their right, and the curly brackets are henceforth omitted to maintain clarity. More generally, we consider a symmetric loading along the crack faces such that

$$\phi_y(x,\pm 0,z)=p(x),\quad x<0 \tag{13}$$

with, again, the assumption that $p(x)$ is zero in a region close to the crack tip. Based on the line load solution, the near-tip field is

$$\phi(x,y,z,t)=\Im\mathfrak{m}P_0\,(x+\mathrm{i}\alpha y)^{\frac{1}{2}}\left[1+\frac{m}{3}(x+\mathrm{i}\alpha y)+\cdots\right], \tag{14}$$

where

$$P_0=\sqrt{\frac{2}{\pi}}\,\frac{K_0}{\alpha},\quad K_0=\sqrt{\frac{2}{\pi}}\int_{-\infty}^{0}\mathrm{d}s\,\frac{p(s)}{(-s)^{1/2}},\quad m=-\frac{1}{K_0}\sqrt{\frac{2}{\pi}}\int_{-\infty}^{0}\mathrm{d}s\,\frac{p(s)}{(-s)^{3/2}}. \tag{15}$$

The amplitude P_0 defines the strength of the square-root 'displacement' behaviour behind the moving tip and K_0 is the analogous scalar 'stress intensity factor', such that the stress ahead of the tip is

$$\phi_y(x,0,z,t)=\frac{K_0}{\sqrt{2\pi x}}\,(1+mx+\cdots). \tag{16}$$

Note that $m=-1$ for the line load limit (10), and the subscript 0 in P_0 and K_0 denotes the displacement and stress coefficients for the unperturbed crack tip at $x=0$. Finally, the scalar energy release rate is

$$G_0=P_0K_0 \tag{17}$$

where, in general,

$$P_0=\lim_{x\uparrow 0}\left[(-x)^{-1/2}\phi(x,0,z,t)\right],\quad K_0=\lim_{x\downarrow 0}\left[\sqrt{x}\,\phi_y(x,0,z,t)\right]. \tag{18}$$

3 Asymptotic solution; scalar model

In the previous section the length scale of the forcing was taken to be much longer than that of the disturbance to the crack tip. This disparity introduces the small parameter ϵ into the problem (in (8b)) which can be usefully employed to solve the problem using the method of matched asymptotic expansions [19]. The non-dimensionalisation carried out previously has cast the initial-boundary-value problem into the 'outer-field' form so we shall have to derive an 'inner' coordinate system too. In the two coordinate systems, asymptotic expansions will be deduced, containing sequences of unknown coefficients, and these will be determined by matching together the respective terms.

3.1 The outer expansion

We begin with the following *ansatz* for the outer expansion

$$\phi(x,y,z,t)=\phi^{(0)}+\epsilon\phi^{(1)}+\epsilon^2\phi^{(2)}+\cdots, \tag{19}$$

where the superscripts in brackets here and henceforth refer to the expansion function at the order in ϵ indicated. Each term in the expansion must satisfy Eq. 8a as well as the crack-face conditions

$$\phi_y^{(n)}(x,\pm 0,z,t)=\delta_{n0}\,p(x),\qquad x<0,\quad n\geq 0, \tag{20}$$

where $\delta_{n0} = 1$ if $n = 0$ and $\delta_{n0} = 0$ otherwise. The leading-order term is the solution for the unperturbed crack,

$$\phi^{(0)} = \Im\mathfrak{m}\, P_0 \left[s^{1/2} + \frac{m}{3} s^{3/2} + \cdots \right], \tag{21}$$

where the complex variable s is

$$s = x + \mathrm{i}\alpha y. \tag{22}$$

The complex form of the solution automatically satisfies a homogeneous crack boundary condition close to the tip. Note that, in terms of the outer coordinates x and y the crack perturbation is very small, hence the reason for locating the centre of the coordinate system at the origin. We will return to the next term in the outer expansion, $\phi^{(1)}$, once we have considered the leading terms in the inner expansion.

3.2 The inner expansion

We introduce dimensionless inner variables X and Y,

$$x = \epsilon X, \quad y = \epsilon Y\,, \tag{23}$$

and let $\Phi(X, Y, z, t) = \phi(x, y, z, t)$. The wave equation expressed in the inner variables is

$$\alpha^2 \Phi_{XX} + \Phi_{YY} + 2\epsilon v \Phi_{Xt} + \epsilon^2 (\Phi_{zz} - \Phi_{tt}) = 0, \tag{24}$$

and the edge is now located at $X = f(z, t)$, $Y = 0$. The inner *ansatz* is motivated by the scaling and by the form of the leading order outer solution:

$$\Phi = \epsilon^{1/2}\, \Phi^{(1/2)} + \epsilon^{3/2}\, \Phi^{(3/2)} + \cdots\,. \tag{25}$$

The leading-order term is easily shown to take the form

$$\Phi^{(1/2)} = \Im\mathfrak{m}\, A^{(1/2)} S^{1/2}, \tag{26}$$

where the inner complex variable S is

$$S = X - f + \mathrm{i}\alpha Y\,, \tag{27}$$

is centred on the perturbed crack tip in order to capture the correct singular behaviour at the shifted edge. The potential $\Phi^{(1/2)}$ satisfies the governing equation (24) with ϵ set to zero (i.e., a scaled form of Laplace's equation) and its derivative is zero on the crack faces as required. The unknown $A^{(1/2)}$ is found by matching the inner and outer expansions. More specifically, we rewrite the inner expansion in terms of the outer variables. Thus, taking Φ up to $\mathcal{O}(\epsilon^{1/2})$, expanding it in terms of the outer variables up to $\mathcal{O}(\epsilon^0)$, and using $S = \epsilon^{-1} s - f$, we obtain

$$\Phi^{\{\frac{1}{2},0\}} = \Im\mathfrak{m}\, A^{(1/2)} s^{1/2}\,. \tag{28}$$

Similarly, the expansion of ϕ up to $\mathcal{O}(\epsilon^0)$ when expressed in terms of the inner variables up to $\mathcal{O}(\epsilon^{\frac{1}{2}})$ is

$$\phi^{\{0,\frac{1}{2}\}} = \epsilon^{1/2}\, \Im\mathfrak{m} P_0 (X + \mathrm{i}\alpha Y)^{1/2}\,. \tag{29}$$

Comparing (28) and (29), we see that they are equivalent if $A^{(1/2)} = P_0$. The next term in the inner expansion satisfies, according to (24) and (25),

$$\alpha^2 \Phi^{(3/2)}_{XX} + \Phi^{(3/2)}_{YY} = -2v \Phi^{(1/2)}_{Xt}\,. \tag{30}$$

The solution is a sum of the particular integral and a general solution. The former is readily found using $\Phi^{(1/2)}_{Xt} = \frac{1}{4} P_0 f_t \Im\mathfrak{m} S^{-3/2}$, combined with the identity $(\alpha^2 \partial_X^2 + \partial_Y^2)\bar{S} g(S) = 4\alpha^2 g'(S)$, where $\bar{S}$ is the conjugate of S. Adding the appropriate general solutions, we determine

$$\Phi^{(3/2)} = \Im\mathfrak{m}\, P_0 \left[A^{(3/2)} S^{3/2} + B^{(3/2)} S^{1/2} + \frac{v}{4\alpha^2} f_t\, \bar{S} S^{-1/2} \right], \tag{31}$$

where $A^{(3/2)}$, $B^{(3/2)}$ are as yet unknown. The expansion of Φ up to $\mathcal{O}(\epsilon^{3/2})$ in outer variables up to $\mathcal{O}(\epsilon^0)$ is therefore,

$$\Phi^{\{\frac{3}{2},0\}} = \mathfrak{Im}\, P_0 \left[s^{1/2} + A^{(3/2)} s^{3/2} \right]. \tag{32}$$

Similarly, from (19) and (21),

$$\phi^{\{0,\frac{3}{2}\}} = \mathfrak{Im}\, P_0 \left[s^{1/2} + \frac{m}{3} s^{3/2} \right]. \tag{33}$$

Comparison of the latter two expansions, which should be identical by the matching rule, implies $A^{(3/2)} = m/3$.

To summarise, the inner solution has been determined to $\mathcal{O}(\epsilon^{3/2})$ as follows,

$$\Phi = \mathfrak{Im} P_0 \left[\epsilon^{1/2} S^{1/2} + \epsilon^{3/2} \left(\frac{m}{3} S^{3/2} + B^{(3/2)} S^{1/2} + \frac{v}{4\alpha^2} f_t\, \bar{s} S^{-1/2} \right) \right] + \mathcal{O}(\epsilon^{5/2}). \tag{34}$$

The single real-valued coefficient $B^{(3/2)}$ remains unknown, and will be found in the next section. Finally, we note for future reference,

$$\Phi^{\{\frac{3}{2},1\}} = \mathfrak{Im}\, P_0 \left[\left(s^{1/2} + \frac{m}{3} s^{3/2} \right) + \epsilon \left[-\tfrac{1}{2} f\, s^{-1/2} + \left(B^{(3/2)} - \frac{m}{2} f \right) s^{1/2} + \frac{v f_t}{4\alpha^2}\, \bar{s} s^{-1/2} \right] \right]. \tag{35}$$

3.3 Wiener–Hopf analysis

In order to proceed to the next order in the outer solution, which is required if we are to match with the inner expansion from (34) it is necessary to consider the perturbation in the wavenumber frequency domain. The most general form of $f(z,t)$ can be constructed from the solution

$$f(z,t) = \mathfrak{Im}\, f_0\, \mathrm{e}^{\mathrm{i}(kz-\omega t)} = \mathfrak{Im} f_0\, \mathrm{e}^{\mathrm{i}\omega(\kappa z - t)}, \tag{36}$$

where $\kappa = k/\omega$ (assumed to be less than unity) is the edge-wave slowness and f_0 is a constant. We seek possible solutions of the outer system of equations with no forcing but which display the singularity represented by the $s^{-1/2}$ term in (35). We therefore assume

$$\phi^{(1)}(x, y, z, t) = \mathfrak{Im}\, q(x, y) \mathrm{e}^{\mathrm{i}\omega(\kappa z - t)}, \tag{37}$$

where $q(x, y)$ satisfies, according to (8),

$$\alpha^2 q_{xx} + q_{yy} + (\omega^2 - k^2) q - 2\mathrm{i}\omega v q_x = 0, \quad -\infty < x < \infty,\ y > 0, \tag{38}$$

and

$$q_y(x, 0) = 0, \quad x < 0, \tag{39a}$$

$$q(x, 0) = 0, \quad x > 0, \tag{39b}$$

$$\lim_{x^2+y^2 \to 0} (x^2 + y^2)^{1/4} q(x, y) < \infty. \tag{39c}$$

One type of general solution is found by a standard analysis involving the Wiener–Hopf method. Thus, let

$$q(x, y) = \frac{1}{2\pi} \int_{-\infty}^{\infty} \mathrm{d}\xi\, \hat{q}(\xi) \mathrm{e}^{-\mathrm{i}\omega\xi x - \omega\gamma y}, \tag{40}$$

where γ follows from (38),

$$\gamma(\xi) = \left(\xi^2 + \kappa^2 - (1 - v\xi)^2 \right)^{1/2}. \tag{41}$$

The integration contour runs along a strip in the complex ξ plane, $\mathcal{D}$ say, which contains the real line except that it is indented above the point $-\lambda_+$ and below the point λ_-, where these correspond to the branch points of γ. The Riemann surface of γ is selected so that $\mathfrak{Re}\, \gamma \geq 0$. We further define

$$\gamma = \gamma^+ \gamma^-, \tag{42}$$

with

$$\gamma^{\pm}(\xi) = \alpha\ (\xi \pm \lambda_{\pm})^{1/2}\,, \qquad \lambda_{\pm} \equiv \frac{1}{\alpha^2}\left(1-\kappa^2\alpha^2\right)^{1/2} \pm \frac{v}{\alpha^2}\,. \tag{43}$$

By definition, the function γ^+ (γ^-) is analytic in the upper (lower) half plane containing the common strip of regularity $\mathcal{D}$. Generally, the superscript notation $\pm$ indicates henceforth functions analytic in these overlapping half-planes.[1] The boundary conditions on $x < 0$ and $x > 0$ imply, respectively,

$$\gamma\hat{q}(\xi) = T^+(\xi), \tag{44a}$$

$$\hat{q}(\xi) = W^-(\xi). \tag{44b}$$

Thus $\gamma^- W^-(\xi)$ and T^+/γ^+ are equal to one another and hence by analytic continuation and Liouville's theorem must be also equal to a constant, say q_0. Therefore, $\hat{q}(\xi) = q_0/\gamma^-(\xi)$.

The near tip behaviour of $q(x, y)$ follows from the behaviour of the transform at large ξ, thus, as $r \to 0$,

$$q(x,y) = \frac{q_0}{2\pi\alpha}\int_{-\infty}^{\infty} \frac{\mathrm{d}\xi\ \mathrm{e}^{-\omega(\mathrm{i}\xi x+|\xi|\alpha y)}}{(\xi-\mathrm{i}0)^{1/2}}\left[1+\frac{\lambda_-}{2\xi}-\frac{1}{2}\alpha y(\lambda_+-\lambda_-)\,\mathrm{sgn}\,\xi+\alpha y(\lambda_++\lambda_-)^2\,\frac{\mathrm{sgn}\,\xi}{8\xi}+\cdots\right]. \tag{45}$$

This can be evaluated using the identities

$$\frac{1}{2\pi}\int_{-\infty}^{\infty} \frac{\mathrm{d}\xi\ \mathrm{e}^{-\omega(\mathrm{i}\xi x+|\xi|\alpha y)}}{(\xi-\mathrm{i}0)^{1/2}\,\xi^n}\left[1,\ \mathrm{sgn}\,\xi\right] = -\frac{2^{2n}n!}{(2n)!}\frac{\mathrm{e}^{\mathrm{i}\pi/4}}{\sqrt{\pi}}(-\mathrm{i})^n\,|\omega s|^{n-\frac{1}{2}}\left[\sin(n-\tfrac{1}{2})\theta\,,\,\mathrm{i}\cos(n-\tfrac{1}{2})\theta\right], \tag{46}$$

for $n \geq 0$, where $s = x + \mathrm{i}\alpha y \equiv |s|\mathrm{e}^{\mathrm{i}\theta}$. Hence,

$$q(x,y) = \frac{q_0}{\alpha}\frac{\mathrm{e}^{\mathrm{i}\pi/4}}{\sqrt{\pi\omega}}\Bigg(|s|^{-1/2}\sin\frac{\theta}{2}+\mathrm{i}\omega\lambda_-|s|^{1/2}\sin\frac{\theta}{2}+\left[\frac{\mathrm{i}}{2}\omega(\lambda_+-\lambda_-)|s|^{1/2}-\frac{\omega^2}{4}(\lambda_++\lambda_-)^2|s|^{3/2}\right] \times\ \sin\theta\cos\frac{\theta}{2}+\cdots\Bigg). \tag{47}$$

Thus, from (37), the second order term in the outer expansion is

$$\phi^{(1)} = \Im\mathfrak{m}\frac{q_0\mathrm{e}^{\mathrm{i}\frac{\pi}{4}}}{\alpha\sqrt{\pi\omega}}\left(|s|^{-\frac{1}{2}}\sin\frac{\theta}{2}+\frac{\mathrm{i}}{4}\omega|s|^{\frac{1}{2}}\left[(\lambda_++3\lambda_-)\sin\frac{\theta}{2}+(\lambda_+-\lambda_-)\sin\frac{3\theta}{2}\right]\right)\mathrm{e}^{\mathrm{i}(kz-\omega t)}+\mathrm{O}(|s|^{\frac{3}{2}})\,. \tag{48}$$

We are now ready to complete the matching with the inner field $\Phi^{\{\frac{3}{2},1\}}$ of (35). This requires that the coefficients of $|s|^{-1/2}\sin\frac{\theta}{2}$, $|s|^{1/2}\sin\frac{\theta}{2}$ and $|s|^{1/2}\sin\frac{3\theta}{2}$, are identically equal. The former implies that

$$q_0 = \tfrac{1}{2}\alpha\sqrt{\pi\omega}\mathrm{e}^{-\mathrm{i}\pi/4}P_0 f_0, \tag{49}$$

while the $|s|^{1/2}\sin\frac{\theta}{2}$ terms match if

$$\begin{aligned} B^{(3/2)} &= \Im\mathfrak{m}\left[\frac{m}{2}+\frac{\mathrm{i}}{8}\omega(\lambda_++3\lambda_-)\right]f_0\mathrm{e}^{\mathrm{i}(kz-\omega t)}\,. \\ &= \Im\mathfrak{m}\left[\frac{m}{2}+\frac{\mathrm{i}}{2\alpha^2}\left(\omega^2-k^2\alpha^2\right)^{1/2}\right]f_0\mathrm{e}^{\mathrm{i}(kz-\omega t)}+\frac{v}{4\alpha^2}f_t, \end{aligned} \tag{50}$$

where $(43)_2$ has been used to express it in a form that will be useful later. Finally, we note that the $|s|^{1/2}\sin\frac{3\theta}{2}$ terms automatically match on account of the identity $(\lambda_+ - \lambda_-) = 2v/\alpha^2$. We are now ready to consider the complete MAE solution.

[1] However, the reader is reminded that the subscript on the constants $\lambda_\pm$ refers only to the choice of sign in (43)!

3.4 Solution and discussion

The strengths of the perturbed singularities at the perturbed crack edge are defined by

$$P \equiv \epsilon^{-1/2} \lim_{X\uparrow 0} |X|^{-1/2}\Phi(X,0,z,t) = P_0 + \epsilon P_0 \left(B^{(3/2)} + \frac{v}{4\alpha^2} f_t \right), \tag{51a}$$

$$K \equiv \epsilon^{-1/2} \lim_{X\downarrow 0} X^{1/2}\Phi_Y(X,0,z,t) = K_0 + \epsilon K_0 \left(B^{(3/2)} - \frac{3v}{4\alpha^2} f_t \right), \tag{51b}$$

where the values follow from the leading-order terms in the inner solution in (34) using (50). Consider the variations from the values for the steadily propagating crack: $\Delta P = P - P_0$, $\Delta K = K - K_0$ and $\Delta G = G - G_0$, where $G = PK$ is the perturbed energy release rate, then the relative changes are

$$\frac{\Delta P}{P_0} = \epsilon g * f + \epsilon \frac{v f_t}{2\alpha^2}, \qquad \frac{\Delta K}{K_0} = \epsilon g * f - \epsilon \frac{v f_t}{2\alpha^2}, \qquad \frac{\Delta G}{G_0} = \epsilon g * f, \tag{52}$$

where $*$ denotes convolution, and the transform of $g(t)$ is

$$\hat{g}(\omega, k) = m + \mathrm{i}\alpha^{-2} \left(\omega^2 - k^2\alpha^2 \right)^{1/2} . \tag{53}$$

The expressions for ΔK and ΔG are identical to analogous ones derived by Woolfries and Willis [8, Eqs. 2.5, 2.7, 2.18]. They also agree with prior work by Rice et al. [1] for the special case of $m = 0$.

Crack-front waves are possible if the phase speed $c_p = \omega/k$ and the crack speed v together lie inside the sonic cone, i.e., they satisfy

$$c_t^2 \equiv v^2 + c_p^2 < 1. \tag{54}$$

In that case the transform $\hat{g}$ becomes

$$\hat{g}(\omega, k) = m - |k| \frac{\sqrt{1 - c_t^2}}{1 - v^2} . \tag{55}$$

Zeros are possible only if m is positive and satisfies

$$0 < m < |k|/\sqrt{1 - v^2}, \tag{56}$$

in which case $\hat{g}(\omega, k)$ has a unique zero at $\omega = \alpha\sqrt{k^2 - \alpha^2 m^2}$. This solution has been discussed before, but we note briefly some properties in the wavenumber domain. The phase speed as a function of k is monotonically increasing from zero at the cutoff or lowest wavenumber possible, $k = m\sqrt{1 - v^2}$, to its asymptote $c_p = \sqrt{1 - v^2}$ as $k \to \infty$. The crack-edge waves are therefore dispersive, and one can, formally at least, define a group speed (velocity), $c_g \equiv \mathrm{d}\omega/\mathrm{d}k$. This is related to the phase speed by

$$c_p c_g = 1 - v^2, \tag{57}$$

and hence, for finite frequency/wavenumber

$$v^2 + c_g^2 > 1. \tag{58}$$

This type of dispersion is anomalous in that the group speed is normally associated with the energy-propagation speed. However, there is no strict connection, and in fact, the notion of energy propagation for edge waves has not been defined. As a result, we may define and calculate c_g although its physical significance is not entirely clear.

It is also of interest to examine the final solution for the near field, as it provides the complete behaviour in the neighbourhood of the moving crack front. Equation (34) implies that the inner solution can be expressed

$$\Phi = P_0 \left(\left[1 + \epsilon \left(\frac{1}{2} g * f + \frac{v f_t}{4\alpha^2} \right) \right] \rho^{1/2} \sin\frac{\Theta}{2} + \left[\frac{m}{3}\rho^{3/2} - \epsilon \frac{v f_t}{4\alpha^2} \rho^{1/2} \right] \sin\frac{3\Theta}{2} \right) + \mathcal{O}(\epsilon^{3/2}), \tag{59}$$

where ρ, Θ are polar coordinates relative to the perturbed moving tip: $x - \epsilon f + \mathrm{i}\alpha y = \rho \mathrm{e}^{\mathrm{i}\Theta}$. We note the appearance of the $\rho^{1/2} \sin\frac{3\Theta}{2}$ term, which affects the stress singularity ahead of the crack, but has a different angular dependence from the standard near tip field $\rho^{1/2} \sin\frac{\Theta}{2}$ for a steadily moving crack.

3.5 Properties of the MAE scheme and simplification

Before considering the elastic crack in detail, we note some general features of the matched asymptotic analysis for the scalar problem. The sequence of terms derived was $\phi^{(0)}$ of (19) $\rightarrow \Phi^{(1/2)}$ of (25) $\rightarrow \Phi^{(3/2)}$ of (34) $\rightarrow \phi^{(1)}$ of (48). The latter was derived as an eigensolution using the Wiener–Hopf method, and was necessary in order to complete the matching of the single remaining coefficient in $\Phi^{(3/2)}$. Note that the particular solution of the inner term for the forcing in Eq. 30 was not required for matching. In fact, the terms in ΔP and ΔK that involve f_t cancel in the final expression for ΔG, i.e., $\hat{g}$ of (53). Thus, we calculated the perturbed values of P and K separately, although the quantity of interest, G, which is their product, turns out to be simpler. This suggests a more direct procedure, which follows by noting that G has alternative expressions:

$$G = PK = \sqrt{\frac{\pi}{2}}\,(1-V^2)^{-1/2}\,K^2 = \sqrt{\frac{2}{\pi}}\,(1-V^2)^{1/2}\,P^2, \tag{60}$$

where $V = v + \epsilon f_t$ is the velocity of the crack edge. The identities (60) are a consequence of the general form of $(15)_1$ for speed V,

$$K = \sqrt{\frac{\pi}{2}}\,(1-V^2)^{1/2}\,P. \tag{61}$$

As a consequence the perturbed energy release rate can be expressed in different ways,

$$\frac{\Delta G}{G_0} = \frac{\Delta P}{P_0} + \frac{\Delta K}{K_0} = 2\frac{\Delta K}{K_0} + \frac{v}{\alpha^2} f_t = 2\frac{\Delta P}{P_0} - \frac{v}{\alpha^2} f_t. \tag{62}$$

Only one or other of P or K needs to be considered in order to calculate the energy-release rate. In practice, it is simpler to compute P as it is the field variable calculated in the MAE procedure. Restricting attention to the crack face $X < 0,\ Y = +0$, and using Eqs. 34 and 35, we have

$$\Phi(-|X|, +0, z, t) = P_0\left[\epsilon^{1/2}(1+\epsilon p_1)|X|^{1/2} - \epsilon^{3/2}\frac{m}{3}|X|^{3/2}\right] + \mathcal{O}(\epsilon^{5/2}), \tag{63}$$

and

$$\Phi^{\{\frac{3}{2},1\}}(-|X|, +0, z, t) = P_0\left[\left(|x|^{1/2} - \frac{m}{3}|x|^{3/2}\right) + \epsilon\left[\tfrac{1}{2} f\,|x|^{-1/2} + \left(p_1 - \frac{m}{2} f\right)|x|^{1/2}\right]\right], \tag{64}$$

where

$$p_1 = B^{(3/2)} + \frac{v f_t}{4\alpha^2} = \epsilon^{-1}\frac{\Delta P}{P_0}. \tag{65}$$

At the same time, the outer expansion evaluated on the crack face is, from (33), (37) and (45),

$$\phi^{\{1,\frac{3}{2}\}} = P_0\left[|x|^{1/2} - \frac{m}{3}|x|^{3/2} + \epsilon\,\Im\mathrm{m}\,\mathrm{e}^{\mathrm{i}(kz-\omega t)}\frac{q_0}{2\pi\alpha}\int_{-\infty}^{\infty}\frac{\mathrm{d}\xi\,\mathrm{e}^{\mathrm{i}\omega\xi|x|}}{(\xi - \mathrm{i}0)^{1/2}}\left(1 + \frac{\lambda_-}{2\xi} + \mathcal{O}(\xi^{-2})\right)\right]. \tag{66}$$

The integral can be evaluated using (46). Matching the $\mathcal{O}(\epsilon)$ terms in (64) and (66), the $|x|^{-1/2}$ singularity gives the identity (49) for q_0, while the next term yields

$$p_1 - \frac{m}{2} f = \Im\mathrm{m}\,\mathrm{i}\omega\frac{\lambda_-}{2} f_0 \mathrm{e}^{\mathrm{i}(kz-\omega t)}. \tag{67}$$

The perturbed energy-release rate then follows from Eqs. 62, 65 and 67.

In summary, we have presented two methods to complete the matching—the first and more general applies the matching to the field $\phi(x, y, z, t)$ for all x and y near the origin, and the second only matches the field on the crack faces, $X < 0,\ Y = 0$. The two methods are equivalent because the final stage of the matching requires only a single real-valued coefficient, and therefore matching of the field along a line amounts to matching over an area (in x and y). However, $B^{(3/2)}$ is not the most relevant quantity for the purpose of calculating the perturbation in the energy-release rate, although this coefficient can be found using the second approach, from Eq. 65 once the coefficient p_1 is known. These same general features are repeated in the elastic case. In particular the calculation of the perturbed energy release rate will be achieved directly once the matching is completed.

4 The elastic crack

We now turn to the more realistic problem of in-plane perturbations of a steadily propagating mode I crack in an isotropic elastic solid. It is important to distinguish between two distinct types of 'crack–edge waves'. The first is the analogue of the Rayleigh surface wave, that is, an infinitesimal wave of particle displacement confined to the edge and decaying away from the edge. The second is a wave-like modification of the edge itself. Achenbach and Gautesen [20] demonstrated the nonexistence of the first type of edge wave on a stationary crack edge. One can show, using their arguments combined with the analysis in the Appendix, that this result extends to a steady propagating crack. That is, there there are no localised solutions of this form for any crack velocity that is subsonic relative to the Rayleigh wave velocity.

4.1 Scaling and asymptotic expansions

The unperturbed crack lies in the plane $y = 0$, with infinite edge moving steadily at speed v, located at $x = 0$, $-\infty < z < \infty$, in the convected coordinate system. We adopt the same scaled coordinates as in the scalar problem, with the distinction that the normalisation in time is with respect to the Rayleigh wave speed c_R, so that the non-dimensional variables are

$$\left(\frac{x - vt}{l}, \frac{y}{l}, \frac{z}{l}, \frac{c_R}{l}t\right) \to (x, y, z, t), \quad \frac{v}{c_R} \to v. \tag{68}$$

The inner and outer expansions for the displacement field $\mathbf{u} = (u_x, u_y, u_z)^T$ are

$$\mathbf{u}(x, y, z, t) = \mathbf{u}^{(0)} + \epsilon\mathbf{u}^{(1)} + \epsilon^2\mathbf{u}^{(2)} + \cdots, \tag{69a}$$

$$\mathbf{U}(X, Y, z, t) = \epsilon^{1/2}\mathbf{U}^{(1/2)} + \epsilon^{3/2}\mathbf{U}^{(3/2)} + \cdots, \tag{69b}$$

where the inner variables X and Y are as the same as before; see Eq. 23. The expansions in (69) are the analogs of those in (19) and (25) for the scalar problem. The boundary conditions on the crack faces are that the traction vector $\boldsymbol{\sigma} = (\sigma_{xy}, \sigma_{yy}, \sigma_{zy})^T$ vanishes, except for the loading, defined below.

We introduce the non-dimensional speeds associated with the two bulk wave speeds in an isotropic elastic medium

$$v_I = c_I/c_R, \quad I = L, T, \tag{70}$$

where $c_L = \sqrt{(\lambda + 2\mu)/\rho_0}$ and $c_T = \sqrt{\mu/\rho_0}$ are the longitudinal and transverse wave speeds, λ and μ are the Lamé moduli and ρ_0 is the mass density. The displacement field is represented by three potentials:

$$\mathbf{u} = \nabla\phi_L + \nabla \wedge \phi_T\mathbf{e}_3 + \nabla \wedge \nabla \wedge \phi_{TH}\mathbf{e}_3, \tag{71}$$

where the L and T are associated with the longitudinal and transverse waves, respectively, and TH is transverse horizontal. The second transverse potential, ϕ_{TH}, is zero in the absence of the perturbation. The effect of changing to the moving coordinate x is that each ϕ_I satisfies a modified wave equation

$$\alpha_I^2\phi_{I,xx} + \phi_{I,yy} + \phi_{I,zz} - \frac{1}{v_I^2}\phi_{I,tt} + 2\frac{v}{v_I^2}\phi_{I,xt} = 0, \quad I = L, T, TH \tag{72}$$

with

$$\alpha_I \equiv \alpha_I(v) = \sqrt{1 - v^2/v_I^2}, \quad I = L, T, \tag{73}$$

and $\alpha_{TH} = \alpha_T$, $v_{TH} = v_T$. The asymptotic analysis will be performed in terms of the potentials, represented as a 3-vector for both the outer and inner regions:

$$\boldsymbol{\phi} \equiv \begin{pmatrix} \phi_L \\ \phi_T \\ \phi_{TH} \end{pmatrix}, \quad \boldsymbol{\Phi} \equiv \begin{pmatrix} \Phi_L \\ \Phi_T \\ \Phi_{TH} \end{pmatrix}, \tag{74}$$

respectively, and which are expanded as

$$\boldsymbol{\phi}(x, y, z, t) = \boldsymbol{\phi}^{(0)} + \epsilon\boldsymbol{\phi}^{(1)} + \epsilon^2\boldsymbol{\phi}^{(2)} + \cdots, \tag{75a}$$

$$\boldsymbol{\Phi}(X, Y, z, t) = \epsilon^{1/2}\boldsymbol{\Phi}^{(1/2)} + \epsilon^{3/2}\boldsymbol{\Phi}^{(3/2)} + \cdots. \tag{75b}$$

4.2 Steadily propagating crack

We first consider solutions for the steadily propagating crack in an isotropic elastic medium. The unperturbed solution has $\phi_{TH} = 0$ and the potentials ϕ_L and ϕ_T may be represented by analytic functions of two complex variables

$$s_I = x + \mathrm{i}\alpha_I y, \qquad I = L,\ T. \tag{76}$$

We introduce the real valued potentials, $\boldsymbol{\psi}_n$, which we express as functions of the complex variables s_L, s_T,

$$\boldsymbol{\psi}_n(s_L, s_T) \equiv \frac{1}{\mu\sqrt{2\pi}\, D(n+\frac{3}{2})(n+\frac{1}{2})}\, \mathfrak{Re} \begin{pmatrix} (1+\alpha_T^2)\, s_L^{n+\frac{3}{2}} \\ \mathrm{i}2\alpha_L\, s_T^{n+\frac{3}{2}} \\ 0 \end{pmatrix}, \tag{77}$$

where

$$D(v) = 4\alpha_L\alpha_T - (1+\alpha_T^2)^2, \tag{78}$$

and $D(1) = 0$ based on the normalisation of the wave speeds with respect to the Rayleigh speed. The associated vectors of displacement and traction are

$$\boldsymbol{\Upsilon}_n = \tfrac{1}{(n+\frac{1}{2})\mu\sqrt{2\pi}\, D}\, \mathfrak{Re}\left[(1+\alpha_T^2)\, s_L^{n+\frac{1}{2}} \begin{pmatrix} 1 \\ \mathrm{i}\alpha_L \\ 0 \end{pmatrix} + \mathrm{i}2\alpha_L\, s_T^{n+\frac{1}{2}} \begin{pmatrix} \mathrm{i}\alpha_T \\ -1 \\ 0 \end{pmatrix} \right], \tag{79a}$$

$$\boldsymbol{\Sigma}_n \ = \tfrac{-1}{\sqrt{2\pi}\, D}\, \mathfrak{Re}\left[(1+\alpha_T^2)\, s_L^{n-\frac{1}{2}} \begin{pmatrix} -2\mathrm{i}\alpha_L \\ 1+\alpha_T^2 \\ 0 \end{pmatrix} + \mathrm{i}2\alpha_L\, s_T^{n-\frac{1}{2}} \begin{pmatrix} 1+\alpha_T^2 \\ 2\mathrm{i}\alpha_T \\ 0 \end{pmatrix} \right]. \tag{79b}$$

We note, in particular, that the zero-traction conditions on the crack face are satisfied.

These fundamental elements may be used to describe a steadily propagating mode I crack, with zero applied shear on the crack faces, i.e., $\sigma_{xy}(x, \pm 0) = \sigma_{zy}(x, \pm 0) = 0$ for $x < 0$. For instance, the solution for a pair of travelling-line loads with $\sigma_{yy}(x, \pm 0) = -\delta(x+1)$ is

$$\sigma_{yy}(x, y) = \frac{1}{\pi D}\, \mathfrak{Re}\left[\frac{4\alpha_L\alpha_T}{(1+s_T)s_T^{1/2}} - \frac{(1+\alpha_T^2)^2}{(1+s_L)s_L^{1/2}} \right]. \tag{80}$$

The near tip fields, in this case, can be expressed terms of the basis functions explicitly as

$$\mathbf{u} = \sqrt{\frac{2}{\pi}} \sum_{n=0}^{\infty} (-1)^n \boldsymbol{\Upsilon}_n, \quad \boldsymbol{\sigma} = \sqrt{\frac{2}{\pi}} \sum_{n=0}^{\infty} (-1)^n \boldsymbol{\Sigma}_n\,. \tag{81}$$

More generally, the loading

$$\sigma_{yy}(x, \pm 0) = -p(x), \quad x < 0, \tag{82}$$

implies a near tip stress expansion identical to that for the scalar problem (see (16))

$$\boldsymbol{\phi} = K_0 \left(\boldsymbol{\psi}_0 + m\boldsymbol{\psi}_1 + \cdots \right) \quad \Leftrightarrow \quad \sigma_{yy}(x, 0) = \frac{K_0 H(x)}{\sqrt{2\pi x}}\, (1 + mx + \cdots). \tag{83}$$

Here K_0 is the stress intensity factor, H is the Heaviside (step) function, and

$$K_0 = \sqrt{\frac{2}{\pi}} \int_{-\infty}^{0} \mathrm{d}s\, (-s)^{-1/2}\, p(s), \qquad m = -\frac{1}{K_0} \sqrt{\frac{2}{\pi}} \int_{-\infty}^{0} \mathrm{d}s\, (-s)^{-3/2}\, p(s). \tag{84}$$

This solution serves as the basis for the perturbed crack.

4.3 Perturbed crack: inner and outer analysis

The leading order term in the outer expansion (75a) is, from (83),

$$\boldsymbol{\phi}^{(0)} = K_0 \left[\boldsymbol{\psi}_0(s_L, s_T) + m\boldsymbol{\psi}_1(s_L, s_T) + \mathrm{O}(s_L^{3/2}, s_T^{3/2}) \right]. \tag{85}$$

Turning to the inner expansion we note that the potentials satisfy modified wave equations

$$\alpha_I^2 \Phi_{I,XX} + \Phi_{I,YY} + \epsilon 2 \frac{v}{v_I^2} \Phi_{I,Xt} + \epsilon^2 \left(\Phi_{I,zz} - \frac{1}{v_I^2} \Phi_{I,tt} \right) = 0, \quad I = L,\ T,\ TH. \tag{86}$$

The leading term in the inner expansion (75b) follows from (85) as

$$\boldsymbol{\Phi}^{(1/2)} = K_0 \, \boldsymbol{\psi}_0(S_L, S_T), \tag{87}$$

where the inner variables are

$$S_I = X - f + \mathrm{i}\alpha_I Y, \quad I = L,\ T. \tag{88}$$

The potentials defined by (87) satisfy the governing equations (86), and the traction conditions on the crack faces.

The potentials in the next term of the inner expansion satisfy the inhomogeneous wave equations

$$\alpha_I^2 \Phi_{I,XX}^{(3/2)} + \Phi_{I,YY}^{(3/2)} = -2 \frac{v}{v_I^2} \, \Phi_{I,Xt}^{(1/2)}, \quad I = L,\ T,\ TH. \tag{89}$$

These may be solved in the same manner as before, as a sum of homogeneous solutions plus the particular solution,

$$\boldsymbol{\Phi}^{(3/2)} = K_0 \left[A^{(3/2)} \boldsymbol{\psi}_1(S_L, S_T) + B^{(3/2)} \boldsymbol{\psi}_0(S_L, S_T) + v f_t \boldsymbol{\psi}_*(S_L, S_T) \right], \tag{90}$$

where the final term is the particular solution given by

$$\boldsymbol{\psi}_*(S_L, S_T) = \frac{1}{\mu \sqrt{2\pi} D} \, \mathfrak{Re} \begin{pmatrix} \dfrac{(1+\alpha_T^2)}{\alpha_L^2 v_L^2} \, \bar{S}_L S_L^{1/2} \\ \dfrac{2i\alpha_T}{\alpha_T^2 v_T^2} \, \bar{S}_T S_T^{1/2} \\ 0 \end{pmatrix}. \tag{91}$$

Matching the outer term $\boldsymbol{\phi}^{\{0,\frac{3}{2}\}}$ with $\boldsymbol{\Phi}^{\{\frac{3}{2},0\}}$ implies that $A^{(3/2)} = m$.

The complete inner solution is therefore

$$\boldsymbol{\Phi} = K_0 \left[\epsilon^{1/2} \boldsymbol{\psi}_0(S_L, S_T) + \epsilon^{3/2} \left(m\boldsymbol{\psi}_1(S_L, S_T) + B^{(3/2)} \boldsymbol{\psi}_0(S_L, S_T) + v f_t \boldsymbol{\psi}_*(S_L, S_T) \right) \right] + \mathcal{O}(\epsilon^{5/2}), \tag{92}$$

from which we can express the expansion of the inner in terms of the outer variable as

$$\begin{aligned} \boldsymbol{\Phi}^{\{\frac{3}{2},1\}} = K_0 \Bigg(& \boldsymbol{\psi}_0(s_L, s_T) + m\boldsymbol{\psi}_1(s_L, s_T) \\ & + \epsilon \left[\frac{1}{2} f \boldsymbol{\psi}_{-1}(s_L, s_T) + \left(B^{(3/2)} - \frac{1}{2} mf \right) \boldsymbol{\psi}_0(s_L, s_T) + v f_t \boldsymbol{\psi}_*(s_L, s_T) \right] \Bigg). \end{aligned} \tag{93}$$

These two equations are the equivalents of (34) and (35) for the perturbed scalar crack model. We note that, as in the scalar problem, the issue is reduced to finding a single real constant, $B^{(3/2)}$.

4.4 Matching and final solution

Based on the experience with the scalar problem, we assume that the $\mathcal{O}(\epsilon)$ outer solution is time-harmonic and of the form

$$\boldsymbol{\phi}^{(1)} = \mathfrak{Re} \, \mathrm{e}^{\mathrm{i}\omega(\kappa z - t)} \, \frac{\omega}{2\pi} \int_{-\infty}^{\infty} \mathrm{d}\xi \, \mathrm{e}^{-\mathrm{i}\omega\xi x} \, \hat{\boldsymbol{\phi}}^{(1)}(\xi, y), \tag{94}$$

where

$$\kappa = 1/c_p \tag{95}$$

denotes the slowness for an assumed edge disturbance with phase speed c_p. The crack-edge perturbation itself is defined by (36). The transform $\hat{\boldsymbol{\phi}}^{(1)}(\xi, y)$ is derived in the Appendix, to within a multiplicative factor. The latter is determined by the near-tip expansion, which is expressed via the large $|\xi|$ behaviour of the transform. Thus, from the Appendix, we have

$$\begin{aligned}\boldsymbol{\phi}^{(1)} &= \mathfrak{Re}\, \mathrm{e}^{\mathrm{i}\omega(\kappa z - t)}\, \frac{\omega}{2\pi} \int_{-\infty}^{\infty} \mathrm{d}\xi\, \mathrm{e}^{-\mathrm{i}\xi x}\, \frac{b_0}{\xi^{3/2}} \begin{pmatrix} -\mathrm{i}(1+\alpha_T^2)\mathrm{e}^{-|\xi|\alpha_L y}(\operatorname{sgn}\xi)\left(1+\mathcal{O}(\xi^{-1})\right) \\ -2\alpha_L \mathrm{e}^{-|\xi|\alpha_T y}\left(1+\mathcal{O}(\xi^{-1})\right) \\ \mathcal{O}(\xi^{-2}) \end{pmatrix} \\ &= \mathfrak{Re}\, \mathrm{e}^{\mathrm{i}\omega(\kappa z - t)}\, b_0 \frac{\mathrm{e}^{-\mathrm{i}\pi/4}}{\sqrt{2}}\, \mu D \left[\boldsymbol{\psi}_{-1}(s_L, s_T) + \mathcal{O}(s_L^{3/2}, s_T^{3/2})\right], \end{aligned} \tag{96}$$

where the identities (46) have been used. The coefficient b_0 is found by matching the coefficient of $\boldsymbol{\psi}_{-1}$ with the $\mathcal{O}(\epsilon)$ term in (93), to give

$$b_0 = \frac{\mathrm{e}^{-\mathrm{i}\pi/4}}{\sqrt{2}} \frac{K_0 f_0}{\mu D}. \tag{97}$$

Hence, the near tip expansion is

$$\boldsymbol{\phi}^{(1)} = \frac{f}{2} K_0 \boldsymbol{\psi}_{-1}(s_L, s_T) + \mathcal{O}(|x|^{3/2}, |y|^{3/2}). \tag{98}$$

The next-order term can be evaluated using the explicit expressions in the Appendix, and in principle the near tip expansion can be continued. However, the leading-order term suffices for our present needs.

The energy-release rate for the perturbed crack front is

$$G = PK = FK^2 = F^{-1}P^2. \tag{99}$$

Here, P and K are defined

$$P \equiv \epsilon^{-1/2} \lim_{X \uparrow 0} \left[|X|^{-1/2} U_y(X, 0, z, t)\right], \quad K \equiv \epsilon^{1/2} \lim_{X \downarrow 0} \left[|X|^{1/2} \Sigma_{yy}(X, 0, z, t)\right], \tag{100}$$

where U_y and Σ_{yy} are the leading-order term in the inner expansion of displacement, (69b), and stress, and [21]

$$F(V) = \frac{2\alpha_L(V) V^2}{v_T^2 \mu D(V)}, \tag{101}$$

with $V = v + \epsilon f_t$. Based on the lessons learned from the scalar problem, we use the final expression in (99) to find the perturbed energy-release rate as

$$\frac{\Delta G}{G_0} = 2\frac{\Delta P}{P_0} - \frac{F'(v)}{F(v)} f_t. \tag{102}$$

Following the procedure for the scalar problem, we can obtain ΔP by matching the crack-opening displacement. Thus,

$$U_y(-|X|, +0, z, t) = \frac{P_0}{\sqrt{2\pi}} \left[\epsilon^{1/2}(1+\epsilon p_1)|X|^{1/2} - \epsilon^{3/2}\frac{m}{3}|X|^{3/2}\right] + \mathcal{O}(\epsilon^{5/2}), \tag{103}$$

and

$$U_y^{\{\frac{3}{2},1\}}(-|X|, +0, z, t) = \frac{P_0}{\sqrt{2\pi}} \left[\left(|x|^{1/2} - \frac{m}{3}|x|^{3/2}\right) + \epsilon \left[\tfrac{1}{2} f\, |x|^{-1/2} + \left(p_1 - \frac{m}{2} f\right)|x|^{1/2}\right]\right], \tag{104}$$

where now

$$p_1 = B^{(3/2)} + \left[\frac{3}{2\alpha_L \alpha_T} + \frac{(1+\alpha_T^2) v_T^2}{4\alpha_L^2 v_L^2}\right] \frac{f_t}{v} = \epsilon^{-1} \frac{\Delta P}{P_0}. \tag{105}$$

The outer expansion for the crack-opening is

$$u_y^{\{1,\frac{3}{2}\}} = \frac{P_0}{\sqrt{2\pi}}\left[|x|^{1/2} - \frac{m}{3}|x|^{3/2} + \epsilon\,\mathfrak{Re}\,\mathrm{e}^{\mathrm{i}(kz-\omega t)}\frac{\omega b_0}{2\pi}\int_{-\infty}^{\infty}\frac{\mathrm{d}\xi\,\mathrm{e}^{\mathrm{i}\omega\xi|x|}}{(\xi-\mathrm{i}0)^{1/2}}\left(1+\frac{a}{\xi}+\mathcal{O}(\xi^{-2})\right)\right], \tag{106}$$

where the complex number a is defined by the expansion of $\hat{u}_y^{(1)}$ in (A.16) and (A.17). Matching the $|x|^{-1/2}$ singularity in the $\mathcal{O}(\epsilon)$ terms in (104) and (106) gives the identity (97), while the $|x|^{1/2}$ coefficient yields

$$p_1 - \frac{m}{2}f = \mathfrak{Im}\,\mathrm{i}\omega a f_0 \mathrm{e}^{\mathrm{i}(kz-\omega t)}. \tag{107}$$

Hence, the transform for the perturbation in energy-release rate, defined by $(52)_3$, is

$$\hat{g}(\omega,k) = m + \mathrm{i}\omega 2a + \mathrm{i}\omega\frac{F'(v)}{F(v)}. \tag{108}$$

This is the fundamental dispersion relation, which will be discussed further in the next section. We note that a similar expression has been obtained by [7, Eq. 4.10], and by [9, Eq. 3.21].[2] However, their expressions differ from (108) in the sign of the second and third terms. This distinction is important for computing the dispersive form of the crack-front wave (see Sect. (5)), but is immaterial in the non-dispersive limit of $m/|k| \to 0$. Finally, we note that the real parameter $B^{(3/2)}$ follows from (105) and (107), and the complete inner expansion to $\mathcal{O}(\epsilon^{3/2})$ is then given by (93).

5 Numerical results and discussion

We discuss solutions to $\hat{g}(\omega,k) = 0$ for $0 < v < 1$, where v is the normalised crack speed relative to the Rayleigh wave speed. Crack-front waves with phase speed $c_p = \omega/k$ lie inside the Rayleigh sonic cone if

$$c^2 = c_p^2 + v^2 < 1, \tag{109}$$

where c is the total speed of the disturbance in the fixed stationary frame. It may be shown [3] that the transform $\hat{g}$ of (108) is real-valued for edge-wave speeds inside the sonic cone. Furthermore, using the change of variables of Ramanathan and Fisher [3], also see [6], we have

$$|k|^{-1}\hat{g}(\omega,k) = \Lambda - 2\frac{\sqrt{1-c^2}}{1-v^2} + \frac{\sqrt{1-c^2/v_L^2}}{1-v^2/v_L^2} + \int_{v_T^2}^{v_L^2}\frac{\mathrm{d}p}{\pi}\,\frac{[2v^2p - c^2(v^2+p)]\beta(p)}{(p-v^2)^2\sqrt{p(p-c^2)}}, \tag{110}$$

where

$$\beta(p) = \tan^{-1}\left(\frac{\sqrt{1-p/v_L^2}\sqrt{p/v_T^2-1}}{\left(1-p/(2v_T^2)\right)^2}\right), \tag{111}$$

and

$$\Lambda = |k|^{-1}m = \frac{\lambda m}{2\pi}. \tag{112}$$

Here λ is the wavelength along the crack, and Λ is therefore the non-dimensional ratio of the wavelength to the length scale of the dynamic loading. At a given crack speed, crack-front waves exist for a range of this parameter: $\Lambda_{\min} < \Lambda < \Lambda_{\max}$, where the lower and upper limits correspond to $c = 1$ and $c = v$, respectively. Thus,

[2] The parameter m used here is the same as that of [9] but twice the value of the quantity m in [7].

$$\Lambda_{\min}(v) = -\frac{\sqrt{1-1/v_L^2}}{1-v^2/v_L^2} - \int_{v_T^2}^{v_L^2} \frac{\mathrm{d}p}{\pi} \frac{(2v^2p - v^2 - p)\beta(p)}{(p-v^2)^2\sqrt{p(p-1)}}, \tag{113a}$$

$$\Lambda_{\max}(v) = \frac{2}{\sqrt{1-v^2}} - \frac{1}{\sqrt{1-v^2/v_L^2}} - \int_{v_T^2}^{v_L^2} \frac{\mathrm{d}p}{\pi} \frac{v^2\beta(p)}{(p-v^2)^{3/2}\sqrt{p}}. \tag{113b}$$

Figure 1 shows $\Lambda_{\min}$ and $\Lambda_{\max}$ as a function of the crack speed for the range of elastic materials, characterised by the Poisson ratio $\nu = (\frac{1}{2}v_L^2 - v_T^2)/(v_L^2 - v_T^2)$, which has the permissible range $-1 < \nu < 0.5$. We note that $\Lambda_{\min}$ is always negative and decreases monotonically to a finite value as $v \to 1$. Note also that $\Lambda_{\max}$ increases monotonically from unity at $v = 0$ and goes as $\Lambda_{\max} \approx 2/\sqrt{1-v^2}$ as $v \to 1$. This behaviour is to be compared with the scalar problem (see Eq. 55) for which $\Lambda_{\min} = 0$ and $\Lambda_{\max} = 1/\sqrt{1-v^2}$. The dependence upon Poisson's ratio is not strong, and therefore for the remainder we consider the single case $\nu = 1/3$.

The phase speed is plotted in Fig. 2 as a function of the crack speed for a range of the non-dimensional wavelength Λ. This extends the results of Morrissey and Rice [6] who presented the $\Lambda = 0$ curve for the total speed c, and of Willis and Movchan [7] who computed the $\Lambda = 0$ curve for the phase speed. Figure 3 shows the total velocity c as a function of v for the same set of Λ. The total speed is always close to unity for negative values of Λ. Thus, $0.995 < c < 1$, $0.987 < c < 1$ and $0.961 < c < 1$ for $\Lambda = -0.4$, -0.2 and 0, respectively. Fig. 4 plots the phase speed as a function of Λ for two values of the crack speed. The range of Λ is consistent with Fig. 1, and note that the lower and upper limiting values of the phase speed correspond to $c = v$ and $c = 1$, respectively. By analogy with the scalar problem, the group speed of the crack-front wave travelling along the edge is defined $c_g = \mathrm{d}\omega/\mathrm{d}k$. It may be shown to be

$$c_g = c_p + \frac{\Lambda}{c_p}\left(\frac{2}{(1-v^2)\sqrt{1-c^2}} - \frac{v_L}{(v_L^2-v^2)\sqrt{v_L^2-c^2}} + \int_{v_T^2}^{v_L^2} \frac{\mathrm{d}p}{\pi} \frac{(c^2v^2 + c^2p - 2p^2)\beta(p)}{(p-v^2)^2(p-c^2)^{3/2}\sqrt{p}}\right)^{-1}, \tag{114}$$

and is plotted in Fig. 5 for a range of values of the wavelength-loading parameter Λ. Note that values of c_g in excess of unity occur, which is highly anomalous. However, in contrast with the scalar case, the group speed does not always satisfy the inequality (58), although it holds more often than not.

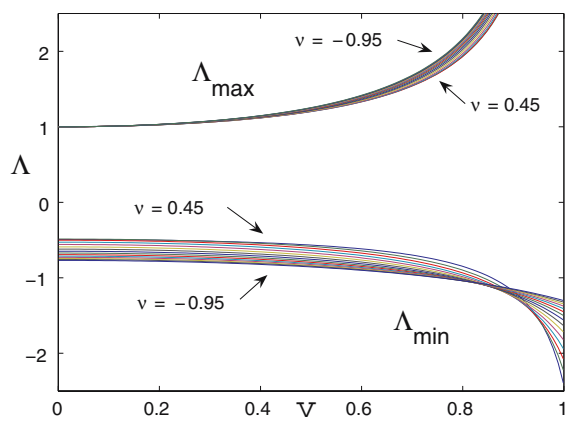

Fig. 1 The limits of the parameter Λ of Eq. 112 as a function of the crack speed. The Poisson ratio of the material ranges from 0.45 to -0.95 in increments of 0.1

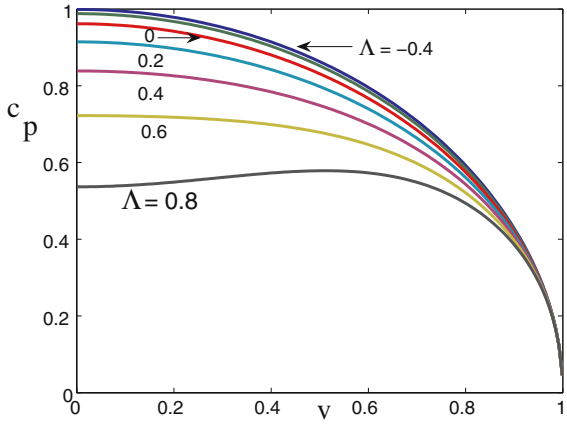

Fig. 2 The crack-front phase speed c_p for $v = 1/3$ vs. the crack-propagation speed for seven values of the non-dimensional wavelength: $\Lambda = -0.4, -0.2, 0, 0.2, 0.4, 0.6$ and 0.8

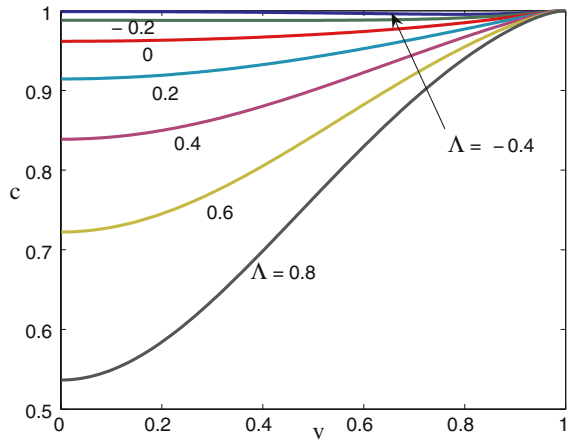

Fig. 3 The total speed of the crack-front wave $c = \sqrt{v^2 + c_p^2}$ vs. the crack-propagation speed for seven values of wavelength: $\Lambda = -0.4, -0.2, 0, 0.2, 0.4, 0.6$ and 0.8

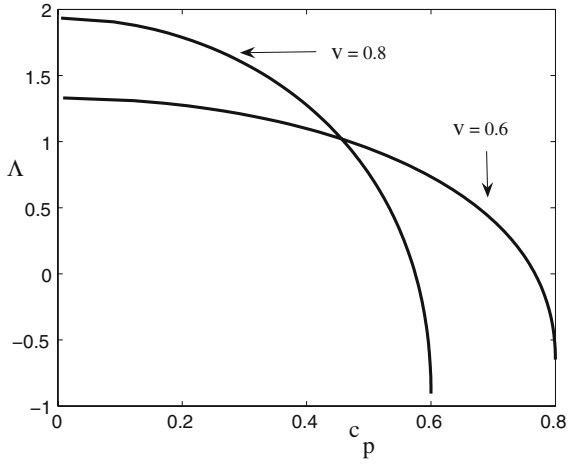

Fig. 4 The dependence of the crack-front phase speed c_p on the non-dimensional wavelength Λ at two values of the crack speed, $v = 0.6$ and $v = 0.8$. The upper limits of c_p in each case are $\sqrt{1 - v^2}$

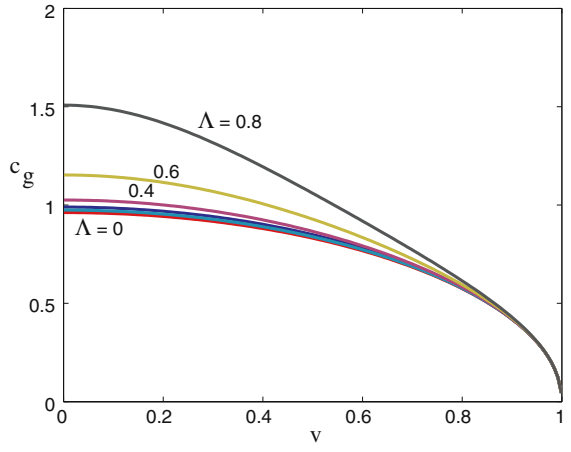

Fig. 5 The group speed c_g of the crack-front wave vs. v for the same set of values for Λ as in Fig. 3

6 Conclusions

We have shown how to solve the scalar model of a perturbed travelling crack edge by using the method of matched asymptotic expansions. The general procedure developed for the model elastic problem was then applied to the elastodynamic mode I crack. The MAE solution employs outer and inner expansions which are matched via the small parameter $\epsilon = L/l$ defined by the disparate length scales: the size L of the edge perturbation and the length scale l associated with the loading. The key to the solution is a homogeneous outer eigensolution which displays unphysical singularities at the unperturbed crack tip. The reason for this is that the crack is shifted, although the unphysical eigensolution is not directly applicable at the crack edge. No unphysical singularities are present in the inner solution, or in the complete matched solution. We have used the MAE scheme to derive the dispersion

relation for the crack-front wave speed, and have shown its dependence on a range of parameters, including crack speed, wavelength, and elastic properties. Once the MAE solution is found to second order in both the inner and outer fields, the dispersion relation is obtained by requiring that the energy release rate, which depends on the inner solution, is unaltered.

The intent of this paper has been to show by example that MAE provides a natural methodology for solving problems of this nature. Future work will develop the procedure to situations that are not easily solved by other means, for instance the perturbation of a dynamic crack front with a cohesive zone at the travelling crack tip. In this case the size of the cohesive zone defines the inner length scale.

Appendix A: Solution of the $\mathcal{O}(\epsilon)$ outer problem

We consider the symmetric boundary-value problem defined by the boundary conditions on $y = 0$:

$$\sigma_{yy} = 0, \quad x < 0, \tag{A.1a}$$

$$u_y = 0, \quad x > 0, \tag{A.1b}$$

$$\sigma_{xy} = \sigma_{zy} = 0, \quad -\infty < x < \infty. \tag{A.1c}$$

This defines a mixed-boundary-value problems on the split regions $x < 0$ and $x > 0$. The solution is assumed in the form (94), and henceforth we will omit the term $\mathrm{e}^{\mathrm{i}\omega(\kappa z - t)}$ and concentrate on the transformed quantities $\hat{\mathbf{u}}^{(1)}(\xi, y)$ and $\hat{\boldsymbol{\sigma}}^{(1)}(\xi, y)$.

The symmetry of the problem implies that we need only consider the half space $y \geq 0$. The transform of the potentials in this half-space may be represented by

$$\hat{\boldsymbol{\phi}}^{(1)} = (\mathrm{i}\omega)^{-1} \begin{pmatrix} A\mathrm{e}^{-\omega\gamma_L y} \\ B\mathrm{e}^{-\omega\gamma_T y} \\ (\mathrm{i}\omega)^{-1} C\mathrm{e}^{-\omega\gamma_T y} \end{pmatrix}, \tag{A.2}$$

and hence the displacement is

$$\hat{\mathbf{u}}^{(1)}(\xi, y) = A(-\xi, \mathrm{i}\gamma_L, \kappa)^T \mathrm{e}^{-\omega\gamma_L y} + \left[B(\mathrm{i}\gamma_T, \xi, 0)^T + C(-\xi\kappa, \mathrm{i}\gamma_T\kappa, \gamma_T^2 - \xi^2)^T \right] \mathrm{e}^{-\omega\gamma_T y}, \tag{A.3}$$

where

$$\gamma_L = \left(\xi^2 + \kappa^2 - \frac{1}{v_L^2}(1 - v\xi)^2 \right)^{1/2}, \quad \gamma_T = \left(\xi^2 + \kappa^2 - \frac{1}{v_T^2}(1 - v\xi)^2 \right)^{1/2}. \tag{A.4}$$

The square-root functions are taken so that $\mathfrak{Re}\,\gamma_L \geq 0$, $\mathfrak{Re}\,\gamma_T \geq 0$, thus ensuring decay in the half-space $y > 0$. The associated stresses follow from (72) and (A.4). The transformed traction, when evaluated on the plane $y = 0$, becomes

$$(\mathrm{i}\omega\mu)^{-1}\hat{\boldsymbol{\sigma}}^{(1)}(\xi, 0) = \begin{bmatrix} -2\mathrm{i}\gamma_L\xi & -\xi^2 - \gamma_T^2 & -2\mathrm{i}\gamma_T\xi\kappa \\ -(\xi^2 + \kappa^2 + \gamma_T^2) & 2\mathrm{i}\gamma_T\xi & -2\gamma_T^2\kappa \\ 2\mathrm{i}\gamma_L\kappa & \xi\kappa & \mathrm{i}\gamma_T(\kappa^2 + \gamma_T^2 - \xi^2) \end{bmatrix} \begin{pmatrix} A \\ B \\ C \end{pmatrix}. \tag{A.5}$$

It is also useful to list the analogous relation for the on-plane displacement transform, from (A.3) with $y = 0$,

$$\hat{\mathbf{u}}^{(1)}(\xi, 0) = \begin{bmatrix} -\xi & \mathrm{i}\gamma_T & -\xi\kappa \\ \mathrm{i}\gamma_L & \xi & \mathrm{i}\gamma_T\kappa \\ \kappa & 0 & \gamma_T^2 - \xi^2 \end{bmatrix} \begin{pmatrix} A \\ B \\ C \end{pmatrix}. \tag{A.6}$$

We are now ready to consider the boundary conditions.

The condition that the stresses σ_{xy} and σ_{zy} vanish on the plane $y = 0$ implies that $\hat{\sigma}^{(1)}_{xy}(\xi, 0) = 0$ and $\hat{\sigma}^{(1)}_{zy}(\xi, 0) = 0$. The first and third rows of the vector relation (A.5) then allows us to eliminate any two of (A, B, C) in favour of the remaining quantity. Substituting the result in the equations for $\hat{\sigma}^{(1)}_{yy}(\xi, 0)$ and $\hat{u}^{(1)}_{y}(\xi, 0)$, we deduce that

$$\hat{\sigma}^{(1)}_{yy}(\xi, 0) = \frac{\omega\mu v_T^2 R}{\gamma_L(1 - v\xi)^2}\, \hat{u}^{(1)}_{y}(\xi, 0), \tag{A.7}$$

where R is the (modified) Rayleigh function

$$R(\xi) = (\xi^2 + \kappa^2 + \gamma_T^2)^2 - 4(\xi^2 + \kappa^2)\gamma_L\gamma_T. \tag{A.8}$$

The boundary conditions (A.1a) and (A.1b) imply that $\hat{\sigma}^{(1)}_{yy}(\xi, 0)$ is a $(+)$ function, i.e., analytic in the upper half of the complex ξ-plane, and $\hat{u}^{(1)}_{y}(\xi, 0)$ is a $(-)$ function. Define

$$Q(\xi) = Q^+(\xi)Q^-(\xi) \equiv \frac{R(\xi)}{(\eta_+ + \xi)(\eta_- - \xi)(\frac{1}{v} - \xi)^2 D}, \tag{A.9}$$

where D is defined in (78) and $\xi = -\eta_+$ and $\xi = \eta_-$ are the zeros of the modified Rayleigh function $R(\xi)$, i.e., the roots of $\xi^2 + \kappa^2 - (1 - v\xi)^2 = 0$,

$$\eta_\pm = \frac{1}{1 - v^2}\left(\sqrt{1 - \kappa^2(1 - v^2)} \pm v\right). \tag{A.10}$$

Thus,

$$Q(\xi) \to 1, \quad |\xi| \to \infty, \tag{A.11}$$

and the functions $Q^\pm(\xi)$ are defined unambiguously by requiring that they both have this property. Using the above mentioned analytic properties of the transforms we may rewrite (A.7) as

$$\frac{\gamma_L^+(\xi)\hat{\sigma}^{(1)}_{yy}(\xi, 0)}{Q^+(\xi)(\eta_+ + \xi)} = \frac{\omega\mu v_T^2 D}{v^2\gamma_L^-(\xi)}\, Q^-(\xi)(\eta_- - \xi)\hat{u}^{(1)}_{y}(\xi, 0) \equiv E(\xi), \tag{A.12}$$

where, by the usual analytic continuation arguments, E is an entire function of the complex variable ξ and

$$\gamma_L^\pm(\xi) = \alpha_L\ (\xi \pm \lambda_{L\pm})^{1/2}, \quad \lambda_{L\pm} = \frac{1}{v_L\alpha_L^2}\left(1 - \kappa^2 v_L^2\alpha_L^2\right)^{1/2} \pm \frac{v}{v_L^2\alpha_L^2}. \tag{A.13}$$

Assume that the stress and displacement behave as

$$u^{(1)}_{y}(x, 0) = \mathcal{O}((-x)^{-1/2}), \quad \sigma^{(1)}_{yy}(x, 0) = \mathcal{O}((-x)^{-3/2}), \tag{A.14}$$

near the edge. This implies that the transforms behave as $\xi^{-1/2}$ and $\xi^{1/2}$ as ξ tends to infinity, and therefore the entire function E is in fact a constant. We assume the constant is non-zero otherwise $\boldsymbol{\phi}^{(1)} = 0$ and the matching cannot be accomplished.

We note that the only non-trivial solution to (A.7) has an unphysical singularity near the edge of the crack. This removes the possibility of infinitesimal localised disturbances, analogous to Rayleigh waves on a free surface. Achenbach and Gautesen [20] considered the possible existence of travelling waves on the edge of a stationary crack, and showed that neither symmetric nor anti-symmetric solutions can exist. Equation A.7 generalises their result to steady propagating cracks, and shows the non-existence of symmetric localized modes. A similar analysis can be done to show that anti-symmetric modes cannot exist on the propagating crack.

In general, the near tip behaviour follows from the expansion of the potentials as $|\xi| \to \infty$. Using

$$Q^-(\xi) = \exp\left(\frac{-1}{2\pi\mathrm{i}}\int_{-\infty}^{\infty} \mathrm{d}\zeta\, \frac{\log Q(\zeta)}{\zeta - \xi}\right), \tag{A.15}$$

we have

$$\hat{u}^{(1)}_{y}(\xi, 0) = \frac{b_0}{\xi^{1/2}}\left[1 + \frac{a}{\xi} + \mathcal{O}(\xi^{-2})\right], \tag{A.16}$$

where, from (A.12) and (A.13),

$$a = \eta_- - \frac{1}{2}\lambda_{L-} - \frac{1}{2\pi \mathrm{i}} \int_{-\infty}^{\infty} \mathrm{d}\zeta \, \log Q(\zeta). \tag{A.17}$$

This is used in Sect. 4 to obtain the perturbed energy-release rate. The detailed form of the inner expansion and the near tip field can be obtained by noting that the explicit form of the potentials are

$$\begin{pmatrix} A \\ B \\ C \end{pmatrix} = \frac{\hat{u}_y^{(1)}(\xi, 0)}{\mathrm{i}\,\gamma_L(\gamma_T^2 - \xi^2)(\xi^2 + \kappa^2 - \gamma_T^2)} \begin{pmatrix} (\xi^2 + \gamma_T^2)(\xi^2 - \kappa^2 - \gamma_T^2) + 2\xi^2\kappa^2 \\ -2\mathrm{i}\xi\gamma_L(\xi^2 + \kappa^2 - \gamma_T^2) \\ 2\kappa\gamma_L\gamma_T \end{pmatrix} \tag{A.18}$$

which imply

$$A = (1 + \alpha_T^2)|\xi|^{-1} \left(1 + \frac{1}{v\xi} \left[\frac{4}{1 + \alpha_T^2} - \frac{(1 - \alpha_L^2)}{\alpha_L^2} \right] + \cdots \right) \hat{u}_y^{(1)}(\xi, 0), \tag{A.19a}$$

$$B = -2\mathrm{i}\alpha_L \xi^{-1} \left(1 + \frac{2}{v\xi} + \cdots \right) \hat{u}_y^{(1)}(\xi, 0), \tag{A.19b}$$

$$C = \frac{2\alpha_L \alpha_T \kappa}{1 - \alpha_T^2} |\xi|^{-3} \left(1 + \frac{1}{v\xi} \left[\frac{1}{\alpha_T^2} + 3 \right] + \cdots \right) \hat{u}_y^{(1)}(\xi, 0). \tag{A.19c}$$

Equations A.16 and A.19 can then be used to derive the near-tip fields.

References

1. Rice JR, Ben-Zion Y, Kim K-S (1994) Three dimensional perturbation solution for a dynamic planar crack moving unsteadily in a model elastic solid. J Mech Phys Solids 42:813–843
2. Perrin G, Rice JR (1994) Disordering of a dynamic planar crack front moving in a model elastic medium of variable toughness. J Mech Phys Solids 42:1047–1064
3. Ramanathan S, Fisher DS (1997) Dynamics and instabilities of planar tensile cracks in heterogeneous media. Phys Rev Lett 79:877–880
4. Willis JR, Movchan AB (1995) Dynamic weight functions for a moving crack. I. mode I loading. J Mech Phys Solids 43:319–341
5. Morrissey JW, Rice JR (1998) Crack front waves. J Mech Phys Solids 46:467–487
6. Morrissey JW, Rice JR (2000) Perturbative simulations of crack front waves. J Mech Phys Solids 48:1229–1251
7. Willis JR, Movchan AB (2001) The influence of viscoelasticity on crack front waves. J Mech Phys Solids 49:2177–2189
8. Woolfries S, Willis JR (1999) Perturbation of a dynamic planar crack moving in a model elastic solid. J Mech Phys Solids 47:1633–1661
9. Woolfries S, Movchan AB, Willis JR (2002) Perturbation of a dynamic planar crack moving in a model viscoelastic solid. Int J Solids Struct 39:5409–5426
10. Obrezanova O, Movchan AB, Willis JR (2002) Dynamic stability of a propagating crack. J Mech Phys Solids 50(12):2637–2668
11. Obrezanova O, Movchan AB, Willis JR (2002) Stability of an advancing crack to small perturbation of its path. J Mech Phys Solids 50(12):57–80
12. Movchan NV, Movchan AB, Willis JR (2005) Perturbation of a dynamic crack in an infinite strip. Quart J Mech Appl Math 58:333–347
13. Bouchaud E, Bouchaud JP, Fisher DS, Ramanathan S, Rice JR (2002) Can crack front waves explain the roughness of cracks. J Mech Phys Solids 50(8):1703–1725
14. Sharon E, Cohen G, Fineberg J (2001) Propagating solitary waves along a rapidly moving crack front. Nature 410:68–71
15. Cohen G, Sharon E, Fineberg J (2002) Crack front waves and the dynamics of a rapidly moving crack. Phys Rev Lett 88(8):085503:1–4
16. Fineberg J, Sharon E, Cohen G (2003) Crack front waves in dynamic fracture. Int J Fract 119:247–261
17. Bonamy D, Ravi-Chandar K (2003) Interaction of shear waves and propagating cracks. Phys Rev Lett 91(23):235502:1–4
18. Willis JR (1999) Asymptotic analysis in fracture: An update. Int J Fract 100:85–103
19. Hinch EJ (1991) Perturbation methods. Cambridge University Press
20. Achenbach JD, Gautesen AK (1977) Elastic surface waves guided by the edge of a slit. J Sound Vib 53(3):407–416
21. Freund LB (1990) Dynamic fracture mechanics. Cambridge University Press